第 48 卷 第 2 期
2021 年 2 月

湖南大学学报（自然科学版）
Journal of Hunan University (Natural Sciences)

Vol. 48. No. 2.
Feb. 2021

Open Access Article

Effect of Austempering Time and Temperature on Microstructure and Phase Fraction of Austempered Ductile Irons

Hoang Anh Tuan[1,2], Nguyen Duong Nam[3], Nguyen Tien Dung[3], Nguyen Huu Dung[2], Nguyen Hong Hai[2]

[1] Technology Institute of Military Department, Ha Noi, Viet Nam

[2] School of Materials Science and Engineering, HUST, Ha Noi, Viet Nam

[3] School of Mechanical Engineering, Vietnam Maritime University, Hai Phong, Viet Nam

Abstract: This article aims to present the results of studying the influence of austempering time and temperature on the microstructure and phase fraction of Austempered Ductile Irons (ADI). The phase fraction in the ADI affects the alloy properties. The research found the best conditions in terms of phase fraction and mechanical properties: the heat treatment process of this alloy is austenitized at 900°C for 2 hours; quenched and held at 780°C for 2 hours; and then austempered at 360°C for various times ranging from 5 to 120 minutes. At this austempering temperature, the higher the Martensite fraction and the lower ausferrite fraction can be obtained. The content of ferrite remains unchanged at the same holding time. When the austempering time increases from 5 to 120 minutes, the content of martensite decreases gradually, whereas the ausferrite phase increases. The ferrite formed in the 2-phase zone has remained without transformation. In the time interval between 90 to 120 minutes, the stable and high carbon ausferrite can be observed (depending on the heat treatment parameters mentioned above). This time domain is called the process window when % M <5%. The resulting mechanical properties show the effect of microstructure and heat treatment process on properties of this alloy.

Keywords: Austempered Ductile Irons, austempering time, phase fraction, dual matrix.

奥氏体时间和温度对奥氏体球墨铸铁组织和相分数的影响

摘要：本文旨在介绍研究奥氏体时间和温度对奥氏体球墨铸铁（阿迪）的组织和相分数的影响的结果。阿迪中的相分数会影响合金性能。研究发现，在相分率和力学性能方面，最佳条件是：该合金的热处理过程在 900 摄氏的温度下奥氏体化 2 小时。淬灭并在 780 摄氏下保持 2 小时；然后在 360 摄氏下回火 5 到 120 分钟。在该奥氏体回火温度下，可以获得较高的马氏体分率和较低的奥氏体分率。在相同的保持时间下，铁素体的含量保持不变。当奥氏体化时间从 5 分钟增加到 120 分钟时，马氏体含量逐渐减少，而奥氏体相增加。在两相区形成的铁素体保持不变。在 90 到 120 分钟之间的时间间隔内，可以观察到稳定的高碳奥氏体（取决于上述热处理参数）。当％中号<5％时，此时域称为过程窗口。所得的机械性能显示出微观结构和热处理工艺对该合金性能的影响。

关键词：奥氏体球墨铸铁，奥氏体时间，相分数，双矩阵。

Received: 4 January 2021 / Revised: 17 January 2021 / Accepted: 18 February 2021 / Published: 28 February 2021

About the authors: Hoang Anh Tuan, Technology Institute of Military Department, Ha Noi, Viet Nam; School of Materials Science and Engineering, HUST, Ha Noi, Viet Nam; Nguyen Duong Nam, Nguyen Tien Dung, School of Mechanical Engineering, Vietnam Maritime University, Hai Phong, Viet Nam; Nguyen Huu Dung, Nguyen Hong Hai, School of Materials Science and Engineering, HUST, Ha Noi, Viet Nam

1. Introduction

Sustainable ADI multiphase matrix is a very attractive material for applications in the mechanical manufacturing industry because a good combination of mechanical properties such as tensile strength and ductility can completely replace cast steel and forged steel; the impact toughness of multiphase matrix ADI is twice higher than normal cast iron, and also has good toughness even at low temperature. The yield of this material is equivalent to forged and cast steel. Although the modulus of elasticity is lower than steel, the damping property of this material is high because of forming the spherical graphite shape. ADI has good casting properties, so it is possible to manufacture gears with different shapes. The casting made from ADI obtains a good surface after the surface treatment process, spraying cleaning balls, and cold deformation. Dual matrix (ferrite + austenite) of ADI is a good selection for driver system and chassis in the defense and automated machinery manufacturing industries because of its mechanical properties such as high yield (~380 up to 550) MPa, high tensile strength (~500 to 900) MPa, good elongation (~14 to 20) %, high impact toughness (~45 to 55) J/cm^2, good corrosion resistance, excellent casting and machinability [1]-[6]. According to [26], the ferrite-ausferrite matrix ductile iron was created by partial austenitization and then austempering. Variation in the ausferrite content was controlled by adding silicon with different content in the studied alloy and kept unchanged the partially austenitizing temperature. The results showed that the strength of the ferrite-ausferrite matrix ductile iron equaled to the strength of peclite matrix cast iron, while the ductility was the same as in the ferrite matrix ductile iron. In the dual matrix (ferrite-ausferrite) ADI, the partial austenitization stage has a strong effect on the mechanical properties because the ferrite and ausferrite fraction in the final structure is controlled at this stage. The influence of the austempering stage on ADI mechanical properties is lower than in conventional ADI [7]-[11]. However, the Bainite reaction mechanism in the cast iron with ferrite-austenite matrix bases on studies on the conventional ADI is also necessary. Ferrite-ausferrite matrix ADI can be produced using the heat treatment process: partial austenitization and then austempering of low alloy ductile iron with ferrite-peclite matrix. The authors demonstrated that (1) hardness increased with raising the austempering temperature, (2) the relation between hardness and yield strength was linear, that means the hardness and the yield increased together, (3) the mechanical properties of the samples were less affected by the austempering temperature, but strongly influenced by the partially austenitizing stage, and (4) the heat treatment process with two steps, austenitization then austempering, improved material properties. The machinability, longevity, and corrosion resistance of ADI were higher than conventional ADI [12]-[16]. Conventional ADI is normally produced by complete austenitization then austempering. In stage I, the main reaction is Ferrite nucleation and growth. Because of the low solubility of carbon in the ferrite, the carbon will be removed from the austenite. Besides, the high concentration of silicon is a reason to delay the carbide precipitation. If this process is stopped at the end of this stage, the stable and high carbon Austenite can be formed after austempering then quenching to room temperature; this leads to a stable ferrite+austenite that called ausferrite. If the heat treatment process is stopped at the end of stage I, the cast iron obtains the best mechanical properties. At stage II – austempering begins with the formation of carbides, then the growth of the Ferrite plates. This means the austenite phase will be decomposed [1], [4], [14]–[21]. The ausferrite morphology depends on the austempering temperature. At high austempering temperature, the low kinetic energy for the reaction and the high diffusion of carbon plays an important role in forming lower bainite ferrite fraction and higher austenite fraction. At lower temperatures, the driving force for the reaction is high, and the diffusion of carbon is very slow, and then more bainite Ferrite and finer bainite ferrite are formed. The perfect microstructure can be obtained after incomplete and rapid austenitization at a temperature in the austenitic region. At high temperatures, the austenite number depends on the austenitizing time, which means the austenite fraction is higher for a longer time. Furthermore, the nucleation and growth of austenite have occurred in the vicinity of graphite particles [1], [22],[23]. The effect of austenitizing temperature and austempering time on the microstructure and tensile strength of austempered ductile iron from the three-phase region was investigated. In this research, ferrite matrix ductile iron was selected for the heat treatment. The authors stated that the increase of the austenitizing temperature led to an increase in the austenite fraction and reduced free ferrite in the 3-phase zone in the final microstructure as described by the phase diagram and the leverage rules. Moreover, high carbon austenite could be formed after this stage. Finally, the austempered materials obtained a higher ductility than conventional ADI and good strength compared to pearlite matrix cast iron [2]. Ferrite matrix

Received: 4 January 2021 / Revised: 17 January 2021 / Accepted: 18 February 2021 / Published: 28 February 2021

About the authors: Hoang Anh Tuan, Technology Institute of Military Department, Ha Noi, Viet Nam; School of Materials Science and Engineering, HUST, Ha Noi, Viet Nam; Nguyen Duong Nam, Nguyen Tien Dung, School of Mechanical Engineering, Vietnam Maritime University, Hai Phong, Viet Nam; Nguyen Huu Dung, Nguyen Hong Hai, School of Materials Science and Engineering, HUST, Ha Noi, Viet Nam

dual iron was used in manufacturing dual-phase ADI. Cast iron was austenitized at about 780°C and 860°C and then austempered at 300°C, 330°C, and 350°C to determine the effects of austenitizing temperature and austempering temperature on microstructure, mechanical properties, and impact toughness. The obtained results show that the mechanical properties were strongly influenced by the partially austenitizing stage, while the austempering tempering had a rather small effect. Increasing the ausferrite fraction in the final microstructure can be improved the mechanical properties of the samples. The suitable hardness was obtained with an ausferrite fraction of about 30%. The carbon content in austenite depended on the temperature of the three-phase zone. For unalloyed ferrite ductile iron, graphite particles were the main sources of carbon. The higher the temperature in austenitizing, the more carbon atoms diffuse from graphite to austenite and dissolve into austenite. As a result, high carbon austenite can be obtained [3],[24]. In the two-step isothermal austempering, by increasing the austempering temperature from 300°C to 380°C, the ausferrite morphology changed from lenticular to feather form, raising high carbon Austenite fraction [12]. Therefore, the ductility and impact toughness increased but reducing the strength and hardness of the cast iron. A study on the mechanical properties of dual-phase ADI from the ferrite matrix ductile iron [15], [26] shows that the appearance and fraction of a new phase after austempering, called new ferrite, affected the material properties. The ductility of the material could be improved by increasing the new ferrite fraction. The dual-phase ADI with 47.2% ausferrite will get a very good combination of tensile strength and elongation, 550 MPa and 25% corresponding. If the ausferrite fraction increase to 75%, tensile strength and elongation can be obtained by 650 MPa and 15%. This material is a good selection of some parts in cars.

The impact strength and elongation increase dramatically, but the tensile strength and elastic limit remain constant in the temperature range from 400°C to 500°C. Beyond this range and the isothermal temperature raise, both tensile strength and elastic limit are decreased. While increasing the temperature in the range of 400-500°C continuously, the impact strength will increase for 90 minutes and then decrease again. The isothermal time is extended at temperatures less than 500°C. The elongation continuously increases for up to 120 minutes, then gradually decreases. At the same time, increasing the isothermal time causes a decrease in the tensile strength and elasticity.

However, the researchers and data about the effects of temperature and time seem to be not interesting. This paper presents the effect of austempering temperature and time on the microstructure and mechanical properties of ADI.

2. Experimental Methodology

In this research, initial ductile iron with a chemical composition in wt.%: 3.6C; 2.44Si; 0.36Mn; 0.89Ni; 0.61Cu; 0.11Cr; 0.015S; 0.0056P and 0.036Mg was produced in a medium frequency induction furnace. The modifier for ductile iron of the Tundish bucket was 2% FeSiMg6 alloy. Denatured anti-white was 0.5% FeSi75. After modification, the melted cast iron was poured into a Y-shaped standard test sample. The pouring temperature was 1450-1480°C. Samples were cut in the lower part of the Y-shaped block. The optical sample size was 15x15x10 mm, and samples of the mechanical test (I-shaped) were prepared according to TCVN 197-1: 2014. For thermal expansion evaluation the specimens were cut into samples of 150 mm in length and 5 mm in diameter.

The microstructure of all samples was evaluated on an optical microscope, Axio Observer D1M (Germany). Matavis Hard software integrated with a microscope was used to determine the phase fraction and microstructure of cast iron. The white ferrite phase, dark martensite, and gray austenite were observed in the microstructure image.

The ductile iron with ferrite and peclite matrix underwent complete austenitization at 900°C for various periods. Then suitable heat treatment parameters were determined to obtain a full austenite matrix in the cast iron.

After that, the samples were moved quickly to another furnace and annealed in the 3-phase zone at 780°C. In this stage, the holding time was enough to ensure that the results of austenite to ferrite transformation reached equilibrium according to the phase diagram. As the calculation, this time was about 1.5-2.0 hours.

The samples were then austempered within a range of 330°C to 420°C with a displacement of 30°C for various times from 0-120 minutes in the salt bath containing 50% KNO_3 + 50% $NaNO_3$. After austempering, the carbon content in ausferrite and mechanical properties were determined. In addition, the thermal expansion of ductile iron and phase fraction was carried out according to the Johnson-Mehl-Avrami formula.

This alloy was studied for such mechanical properties as strength and hardness.

3. Results and Discussion

3.1. Microstructure

When studying microstructure, it can be seen the large number and concentrate of martensite in austempered samples after holding 5 minutes, 15 minutes, and 30 minutes. The first appearance of acicular ferrite and high carbon ausferrite can be observed at the boundaries of martensite and ferrite. The martensite fraction was still high when the austempering time was kept to 60 minutes and 90 minutes. Moreover, this phase was still observed after austempered for 120 minutes.

According to the austempering time, the multiphase software was used to determine the volume fraction of ferrite, martensite, and ausferrite. The results are shown in Table 1.

Table 1 The phase fraction after heat treatment at 900°C, 780°C, 330°C for various times

Time (min)		5	15	30	60	90	120
Phase fraction %	Ausferrite	4.3	11.6	18.5	34.5	48.4	58.4
	Martensite	55.7	48.4	41.2	25.3	11.3	1.2
	Ferrite	40.0	40.0	40.3	40.2	40.3	40.4

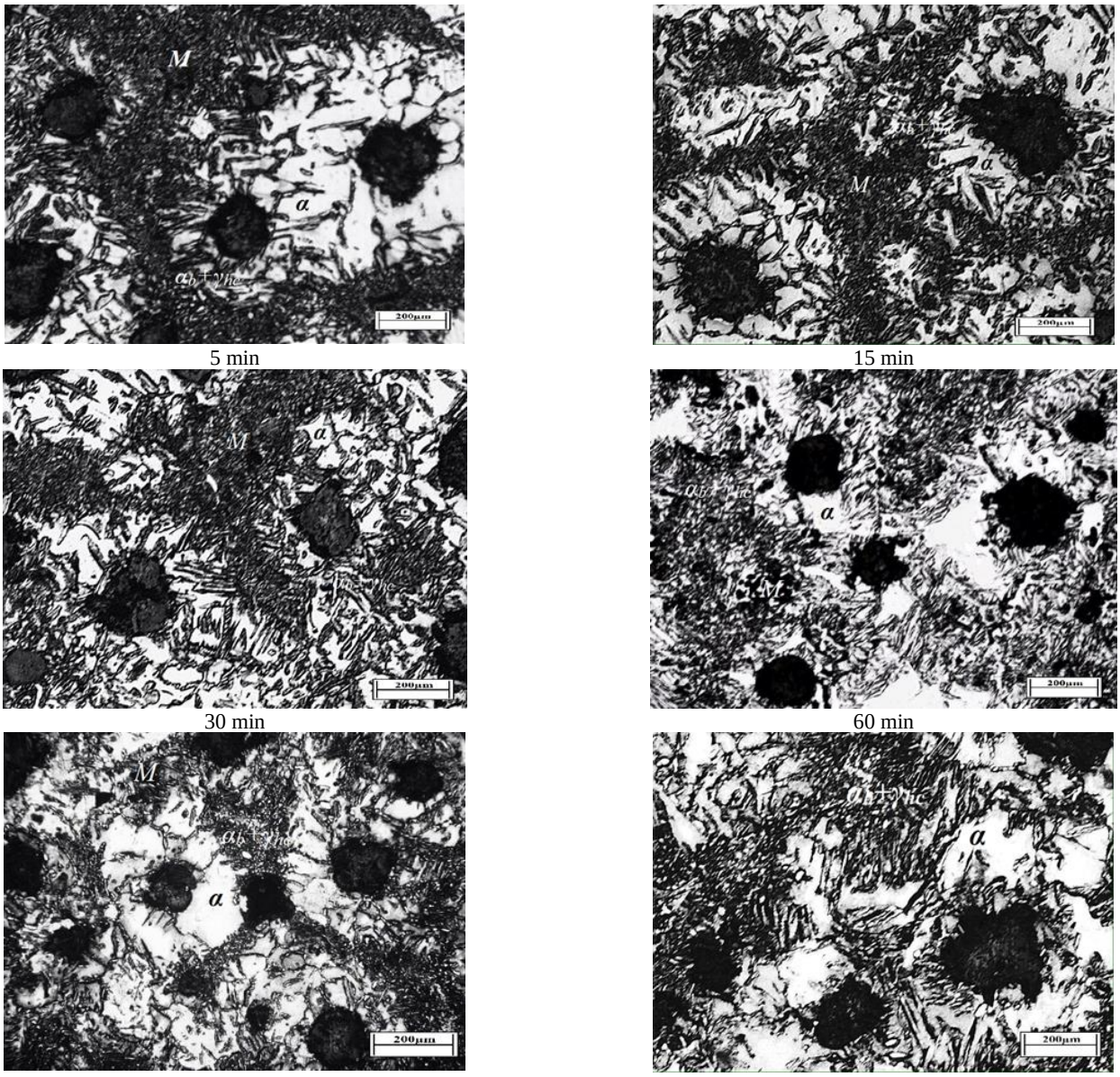

5 min | 15 min | 30 min | 60 min | 90 min | 120 min

Fig. 1 Microstructure of ductile iron after heat treatment: austenitized at 900°C for 2 hours; quenched and held at 780°C for 2 hours, and then austempered at 360°C

From optical micrographs, it can be seen the large number and concentrate of Martensite in austempered samples after holding 5 minutes, 15 minutes, and 30 minutes. The first appearance of acicular ferrite and high carbon ausferrite can be observed at the boundaries of Martensite and Ferrite. The Martensite phase remained when the austempering times were 60 minutes and 90 minutes. Moreover, no Martensite can be observed after austempered for 120 minutes. The matrix structure, in this case, was Ferrite and Ausferrite ($\alpha_b + \gamma_{hc}$). From this point, the microstructure remained stable and uniform when increasing austempering time.

Table 2 The phase fraction after heat treatment at 900°C, 780°C, 360°C for various times

Time (min)		5	15	30	60	90	120
Phase fraction %	Ausferrite	6.5	14.1	20.3	35.8	51.5	59.1
	Martensite	53.3	45.6	39.4	23.4	8	0
	Ferrite	40.2	40.3	40.3	40.8	40.5	40.9

These results were used in the ADI microstructures rating chart (austenitized at 900°C for 2 hours; quenched and held at 780°C for 2 hours, and then austempered at 360°C for various times from 5 to 120 minutes).

The heat treatment process in table 3 shows the medium number and concentrate of martensite in austempered samples after holding 5 minutes, 15 minutes, and 30 minutes. The first appearance of acicular ferrite and high carbon ausferrite can be observed at the boundaries of martensite and ferrite. The small number of martensite phase was remained after holding 60 minutes and 90 minutes. Moreover, no martensite can be observed after austempered for 120 minutes. The ferrite and ausferrite matrix structure ($\alpha_b + \gamma_{hc}$) was obtained.

Table 3 The phase fraction after heat treatment at 900°C, 780°C, 390°C for various times

Time (min)		5	15	30	60	90	120
Phase fraction %	Ausferrite	10	19.3	28.3	47.1	55	59.4
	Martensite	49.9	40.6	31.4	12.4	4.5	0
	Ferrite	40.1	40.1	40.3	40.5	40.5	40.6

After heat treatment at 900°C, 780°C, 420°C for various times that the medium number and concentrate of martensite in austempered samples can be observed after holding 5 minutes, 15 minutes, and 30 minutes. The first appearance of acicular ferrite and high carbon ausferrite can be observed at the boundaries of martensite and ferrite. The martensite phase remained when the austempering times were 60 minutes. Moreover, no martensite can be observed after austempered for 90 minutes and 120 minutes. The matrix structure, in this case, was ferrite and ausferrite ($\alpha_b + \gamma_{hc}$). From 90 minutes and longer, the microstructure remained stable and uniform.

Table 4 The phase fraction after heat treatment at 900°C, 780°C, 420°C for various times

Time (min)		5	15	30	60	90	120
Phase fraction %	Ausferrite	10.8	20.2	29.4	48	55.4	59.4
	Martensite	49.1	39.7	30.3	11.5	4.1	0
	Ferrite	40.1	40.1	40.3	40.5	40.5	40.6

Figure 2 shows the changes in microstructure and phase fraction, which depended on temperature and austempering time. With the small difference in ferrite fraction at various temperatures, this value can be viewed equally in the austempering processes.

The chart shows that the ferrite fraction unchanged in all samples. The Martensite fraction was higher at lower austempering temperature, and the Ausferrite fraction was lower at higher austempering temperature. The higher the Martensitic volume fraction change, the longer the process of microstructural stabilization. The lower appearance of the process window can occur (as calculated when% M <5%).

At the austempering temperature of 390°C, 420°C, the change in phase fraction is relatively large at first, but after holding 60 minutes, the microstructure remained

stable. The process window was also located at a 90 – 120-minute interval.

The austenitized samples were quenched from the 3-phase zone (α+γ+graphite) to the austempered zone. The samples with original phases of the matrix were α+γ were austempered and then cooled to room temperature close to the M_S point line. At this stage: the first phase transformation occurred with the forming of acicular ferrite, the residual carbon diffused into the austenite and obtained high carbon austenite and became more stable ($\gamma \rightarrow \alpha b + \gamma HC$), this phase has been called Ausferrite. However, if quenching to room temperature, low carbon austenite transformed to Martensite, which caused increased hardness value, wear-resistance, and reduced ductility of cast iron. On the other hand, because the specific volume of ferrite is higher than ausferrite, the ausferrite has more carbon content and more stable and difficult transformation. If the austempering time is too short (< 90 minutes), the Ausferrite stability is not high when quenching below M_S, and the austenite transformed to martensite.

With increasing austempering time, the number of the martensite reduces, whereas the ausferrite fraction increase. the ferrite fraction that formed in the 2-phase zone remains unchanged with no transformation.

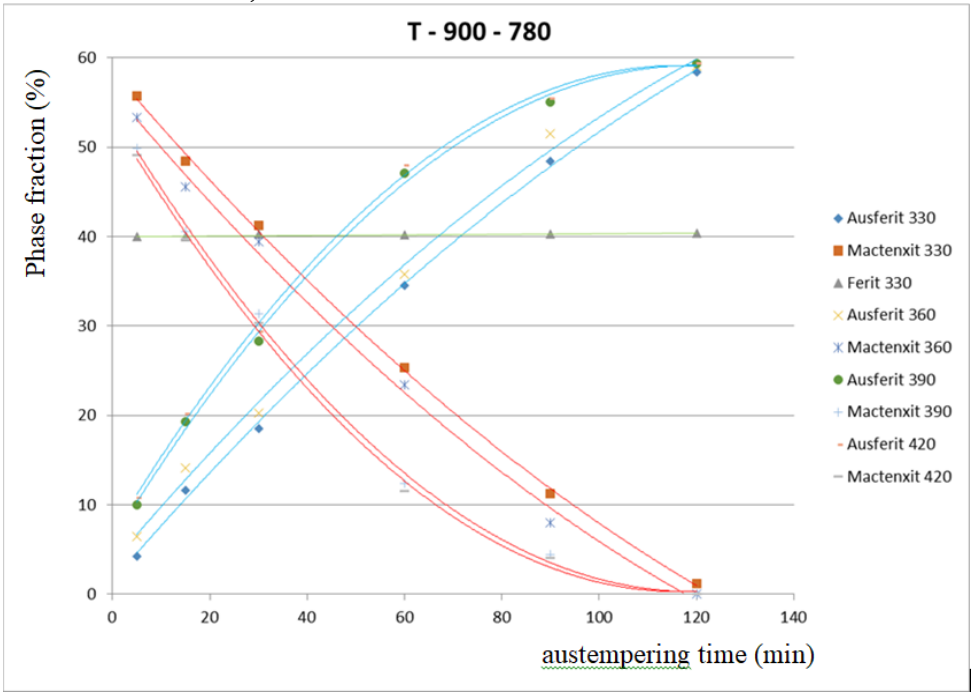

Fig. 2 ADI microstructures rating chart (austenitized at 900°C for 2 hours; quenched and held at 780°C for 2 hours)

When the austempering time was about 120 minutes, there was no presence or small martensite volume fraction. The matrix structure of cast iron included ferrite and ausferrite. At this time, the austenite of rich in carbon and very stable, so the austenite to martensite transformation will not occur when quenching to room temperature. After 120 minutes, the austenitic became more stable and richer in carbon. Thus, the reaction $\gamma \rightarrow \alpha_b + \gamma_{HC}$ occurred at the end of stage I. The carbon-rich austenite is very stable and does not change, and this time domain is called a "process window". The process window started from the point of martensite fraction less than 5%. Figure 2 shows that the process window depends on the heat treatment parameters as mentioned above.

As can be seen from Figure 3 and Table 5, the hardness of ductile iron with a fully ausferrite matrix structure is higher than material with traditional heat treatment. The dual-phase ADI properties are different from traditional cast iron because of the dual matrix structure (ausferrite and ferrite). The ADI with better ductility and lower hardness is a good material for many applications in life.

Table 5 Phase fraction and hardness of traditional ADI and dual-phase ADI

Samples	**Phase fraction of Ausferrite %**	**Ferrite fraction %**	**Hardness HB**
Traditional ADI	100	0	325
Dual-phase ADI	59.4	40.6	246

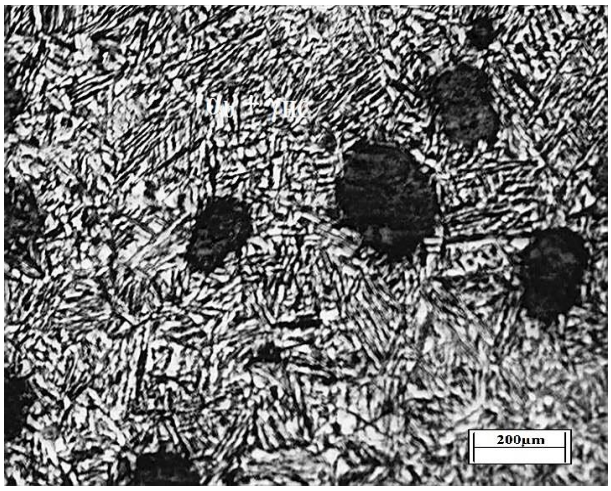

a) Traditional ADI

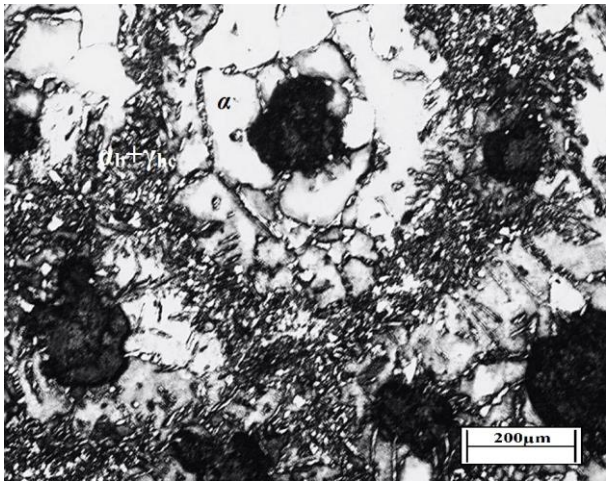

b) Dual-phase ADI

Fig. 3 Microstructure of ADI: a) traditional ADI: austenitized at 900°C for 2 hours; quenched and held at 360 ^{0}C for 2 hours b) dual-phase ADI austenitized at 900 ^{0}C for 2 hours; quenched and held at 780 ^{0}C for 2 hours; and then austempered at 360 ^{0}C for 2 hours

3.2. Mechanical Properties

Figure 4 presents the hardness of the samples after heat treatment. In stage I, the time interval 5 to 120 minutes occurring the reaction ($\gamma \rightarrow \alpha_b + \gamma_{HC}$), the hardness of samples decrease with increasing the austempering time. The reason is that the phase transformation leads to reduces Martensite fraction in this stage. The highest hardness can be obtained after quenching for 5 minutes, corresponding to the maximum Martensite fraction.

In the process window of 120 minutes, the hardness values increase with increasing austempering time. There is no transformation in this region, but increasing austempering time leads to the austenitic phase more stable, high carbon content, and the hardness of this phase will increase, leading to a change in the hardness of the sample.

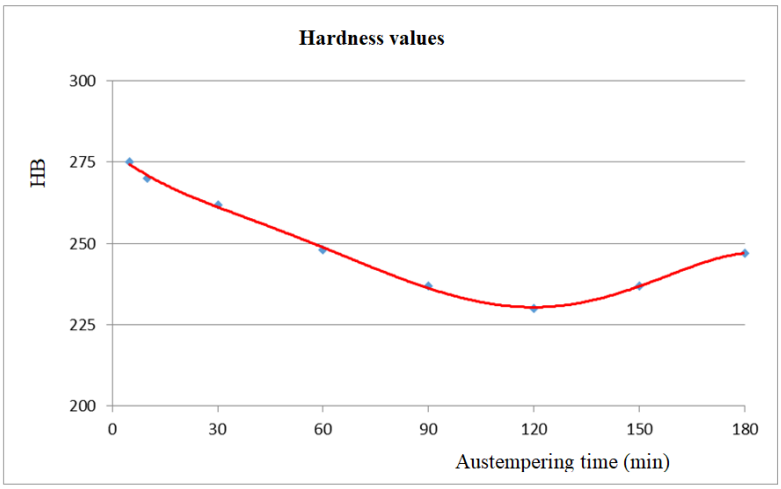

Fig. 4 Hardness values of austempered samples at various times

Table 6 The strength and elongation austenitized at 900^{0}C for 2 hours; quenched and held at 780^{0}C for 2 hours; and then austempered at 360^{0}C at various times

No.	Sample No.	Heat treatment process	Properties		
			Tensile strength Rm, MPa	Yield strength Rp0.2, MPa	A, %
01	M7	900-2h-780 – 2h _360-30 min	823	588	14.4
02	M8	900-2h-780 – 2h _360-60 min	816	582	14.3
03	M9	900-2h-780 – 2h _360-90 min	846	604	13.1

04	M10	900-2h-780 – 2h _360-120 min	854	606	12.3
05	M11	900-2h-780 – 2h _360-150 min	860	614	11.0
06	M12	900-2h-780 – 2h _360-180 min	861	616	10.4

In table 6, when increasing austempering time, the tensile and yield strength increase, from 30 to 90 min the value of elongation decreases slowly (from 14.4 to 13.1%), but from 120 to 180 min, this value decreases quickly (from 12.3 to 10.4%).

4. Conclusions

The table of ferrite and martensite fraction depending on time and temperature in a critical zone is built. It can be seen that the higher the heating temperature and lower holding time, the content of ferrite reduces after heat treatment. The ferrite fraction plays an important role in the mechanical properties of cast iron. The cast iron with higher ferrite content obtains a good combination of ductility, tensile strength, and hardness. Therefore, based on the mechanical requirements, it is possible to select a suitable thermal treatment technology process corresponding to the ferrite fraction in the cast iron.

ADI dual matrix can be produced after heat treatment as follows: austenitized at 900°C for 2 hours; and quenched and held at 780°C for 2 hours; and then austempered at 360°C for various times of 5 to 120 minutes. The lower the austempering temperature is, the higher the martensite fraction and the lower ausferrite fraction can be obtained. The ferrite content remains unchanged at the same holding time. When the austempering time increases from 5 to 120 minutes, the martensite content decreases gradually, whereas the ausferrite phase increases. the ferrite formed in the 2-phase zone has remained without transformation. In the time interval between 90 to 120 minutes, the stable and high-carbon ausferrite can be observed (depending on the heat treatment parameters mentioned above). This time domain is called the process window when % M <5%.

It is noticed that the lower temperature in the critical temperature zone, the higher ferrite and the lower ausferrite fraction. After quenching, the ausferrite and martensite fractions reduce compared to the samples heated in the high critical temperature zone. At the same temperature, the hardness values of austempered samples decrease with increasing the austempering time from 0 to 120 min. However, with increasing time, the hardness increases, but the strength values increase when increasing the austempering time. However, the elongation decreases when increasing the austempering time.

The novelty in this study indicates the influence of austempering temperature and time on the microstructure, phase fraction, and properties of research alloys. This new point in references has not been announced before. Based on the research results, the heat treatment process was determined to control the alloy microstructure in accordance with different purposes.

References

[1] GÓRNY M, ANGELLA G, TYRAŁA E, *et al*. Role of Austenitization Temperature on Structure Homogeneity and Transformation Kinetics in Austempered Ductile Iron. *Metals and Materials International*, 2019, 25(4): 956-965. https://doi.org/10.1007/s12540-019-00245-y.

[2] KILICLI V, & ERDOGAN M. Effect of ausferrite volume fraction and morphology on tensile properties of partially austenitised and austempered ductile irons with dual matrix structures. *International Journal of Cast Metals Research* 2007, 20(4): 202-2014. https://doi.org/10.1179/136404607X256051

[3] DONNINI R, FABRIZI A, BONOLLO F, *et al*. Assessment of the microstructure evolution of an austempered ductile iron during austempering process through strain hardening analysis. *Metals and Materials International* 2017, 23(5): 855-864. https://doi.org/10.1007/s12540-017-6704-y

[4] ZHANG H, WU Y, LI Q, & HONG X. Mechanical properties and rolling-sliding wear performance of dual phase austempered ductile iron as potential metro wheel material. *Wear*, 2018, 406-407(April): 156-165. https://doi.org/10.1016/j.wear.2018.04.005

[5] WANG B, BARBER GC, TAO C, *et al*. Characteristics of tempering response of austempered ductile iron. *Journal of Materials Research and Technology*, 2018, 7(2): 198-202. https://doi.org/10.1016/j.jmrt.2017.08.011

[6] KIM YJ, SHIN H, PARK H, *et al*. Investigation into mechanical properties of austempered ductile cast iron (ADI) in accordance with austempering temperature. *Materials Letters*, 2008, 62(3): 357-360. https://doi.org/10.1016/j.matlet.2007.05.028.

[7] ERIĆ O, JOVANOVIĆ M, ŠIDANIN L, *et al*. The austempering study of alloyed ductile iron. *Materials and Design* 2006, 27(7): 617-622. https://doi.org/10.1016/j.matdes.2004.11.028

[8] HEGDE, A., SHARMA, S., & VIKAS SADANAND, R. Mechanical characterization and optimization of heat treatment parameters of manganese alloyed austempered ductile iron. *Journal of Mechanical Engineering Science*, 2019, 13(1): 4356-4367. https://doi.org/10.15282/jmes.13.1.2019.01.0371

[9] HEGDE, A., SHARMA, S., & SHANKAR M. C. Machinability and related properties of austempered ductile iron: A review. *Journal of Mechanical Engineering Science*, 2018, 12(4): 4180-4190. https://doi.org/10.15282/jmes.12.4.2018.14.0360

[10] WANG B, BARBER G, SUN X, *et al*. Characteristics of the Transformation of Retained Austenite in Tempered Austempered Ductile Iron. *Journal of Materials Engineering and Performance*, 2017, 26(5): 2095-2101. https://doi.org/10.1007/s11665-017-2663-1

[11] KILICLI V. & ERDOGAN M. Effect of ausferrite volume fraction and morphology on tensile properties of partially austenitised and austempered ductile irons with dual matrix structures. *International Journal of Cast Metals Research*, 2007, 20(4):202-214.
[12] SETHURAM D, SRISAILAM S, & PONANGI BR. Sliding wear and corrosion behaviour of alloyed austempered ductile iron subjected to novel two step austempering treatment. *IOP Conference Series: Materials Science and Engineering*, 2018, 346(1). https://doi.org/10.1088/1757-899X/346/1/012035
[13] TARAN YN, UZLOV KI, & KUTSOV AY. The bainite reaction kinetics in austempered ductile iron. *Journal de Physique IV*, 1997, 7(5). https://doi.org/10.1051/jp4:1997568
[14] KILICLI V, & ERDOGAN M. The strain-hardening behavior of partially austenitized and the austempered ductile irons with dual matrix structures. *Journal of Materials Engineering and Performance* 2008, 17(2): 240-249. https://doi.org/10.1007/s11665-007-9143-y
[15] SELLAMUTHU P, SAMUEL DGH, DINAKARAN D, *et al*. Austempered ductile iron (ADI): Influence of austempering temperature on microstructure, mechanical andwear properties and energy consumption. *Metals (Basel)*, 2018, 8(1), 53: 1-12. https://doi.org/10.3390/met8010053
[16] SAHIN Y, ERDOGAN M, & KILICLI V. Wear behavior of austempered ductile irons with dual matrix structures. *Materials Science and Engineering: A*, 2007, 444(1-2): 31-38. https://doi.org/10.1016/j.msea.2006.06.071
[17] DONG BX, QIU F, LI Q, *et al*. The synthesis, structure, morphology characterizations and evolution mechanisms of nanosized titanium carbides and their further applications. *Nanomaterials*. 2019, 9(8): 1152. https://doi.org/10.3390/nano9081152
[18] ČATIPOVIĆ N, ŽIVKOVIĆ D, & DADIĆ Z. The effects of molybdenum and manganese on the mechanical properties of austempered ductile iron. *Tehnički Vjesnik*, 2018, 25(2): 635-642. https://doi.org/10.17559/TV-20170124120729
[19] ŁAWRYNOWICZ, Z. & DYMSKI, S. Analysis of carbon partitioning during ausferritic reaction in ADI. *Archives of Foundry Engineering*, 2008, 8(3): 69-74.
[20] DAKRE V, PESHWE DR, PATHAK SU, *et al*. Mechanical Characterization of Austempered Ductile Iron Obtained by Two Step Austempering Process. *Transactions of The Indian Institute of Metals* 2017, 70(9): 2381-2387. https://doi.org/10.1007/s12666-017-1099-5
[21] BOCCARDO AD, DARDATI PM, GODOY LA. Influence of alloy element distributions on austempered ductile irons. *Materials Science and Technology (United Kingdom)*, 2018, 34(17): 2153-2165. https://doi.org/10.1080/02670836.2018.1521062
[22] CHENG H, FU H, MA S, *et al*. Effects of austenitizing process on microstructures and properties of carbidic austempered ductile iron. *Materials Research Express*, 2019, 6(1). https://doi.org/10.1088/2053-1591/aae44c
[23] MOZUMDER YH, BEHERA RK, & SEN S. YH. Influence of Intercritical Austenitizing Temperature, Quenching Media and Tempering Temperature on Mechanical Properties and Wear Behavior of Ductile Iron with Dual Matrix Structure. *Orissa Journal of Physics*, 2015, 22(1): 39-51.
[24] TYRAŁA E, GÓRNY M, KAWALEC M, *et al*. Evaluation of volume fraction of austenite in austempering process of austempered ductile iron. *Metals (Basel)*. 2019, 9(8). https://doi.org/10.3390/met9080893
[25] YANG J, & PUTATUNDA SK. Influence of a novel two-step austempering process on the strain-hardening behavior of austempered ductile cast iron (ADI). *Materials Science and Engineering: A*, 2004, 382(1-2): 265-279. https://doi.org/10.1016/j.msea.2004.04.076
[26] ARANZABAL J, SERRAMOGLIA G, GORIA CA, *et al*. Development of a new mixed (ferritic-ausferritic) ductile iron for automotive suspension parts. *International Journal of Cast Metals Research*, 2003, 16(1-3): 185-190, https://doi.org/10.1080/13640461.2003.11819580

参考文:

[1] GÓRNY M，ANGELLA G，TYRAŁAE 等。奥氏体化温度对奥氏体球墨铸铁组织同质性和转变动力学的影响。金属与材料国际，2019，25（4）：956-965。https://doi.org/10.1007/s12540-019-00245-y。
[2] KILICLI V 和 ERDOGAN M。奥氏体体积分数和形态对具有双基体结构的部分奥氏体化和奥氏体球墨铸铁的拉伸性能的影响。国际铸造金属研究杂志 2007，20（4）：202-2014。https://doi.org/10.1179/136404607X256051
[3] DONNINI R，FABRIZI A，BONOLLO F 等。通过应变硬化分析评估奥氏体球墨铸铁在奥氏体回火过程中的组织演变。金属与材料国际 2017，23（5）：855-864。https://doi.org/10.1007/s12540-017-6704-y
[4] ZHANG H, WU Y, LI Q, 和 HONG X。双相奥氏体球墨铸铁作为潜在的地铁车轮材料的力学性能和滚动滑动磨损性能。磨损，2018，406-407（4 月）：156-165。https://doi.org/10.1016/j.wear.2018.04.005
[5] WANG B，BARBER GC，TAO C 等。奥氏体球墨铸铁的回火特性。材料研究与技术学报，2018，7（2）：198-202。 https://doi.org/10.1016/j.jmrt.2017.08.011
[6] KIM YJ，SHIN H，PARK H 等。根据奥氏体温度研究奥氏体球墨铸铁（阿迪）的力学性能。材料快报，2008，62（3）：357-360。https://doi.org/10.1016/j.matlet.2007.05.028。

[7] ERIĆ O，JOVANOVIĆ M，ŠIDANIN L 等。合金球墨铸铁的奥氏体研究。材料与设计 2006，27（7）：617-622。https://doi.org/10.1016/j.matdes.2004.11.028
[8] HEGDE，A.，SHARMA，S。和 VIKAS SADANAND，R。锰合金奥氏体球墨铸铁的力学特性和热处理参数的优化。机械工程学报，2019，13（1）：4356-4367。https://doi.org/10.15282/jmes.13.1.2019.01.0371
[9] HEGDE，A.，SHARMA，S. 和 SHANKAR M. C. 奥氏体球墨铸铁的可加工性和相关性能：综述。机械工程学报，2018，12（4）：4180-4190。https://doi.org/10.15282/jmes.12.4.2018.14.0360
[10] WANG B，BARBER G，SUN X 等。回火奥氏体球墨铸铁中残余奥氏体的转变特征。材料工程与性能，2017，26（5）：2095-2101。 https://doi.org/10.1007/s11665-017-2663-1
[11] KILICLI V. 和 ERDOGAN M. 奥氏体体积分数和形态对具有双基体结构的部分奥氏体和奥氏体球墨铸铁的拉伸性能的影响。国际铸造金属研究杂志，2007，20（4）：202-214。
[12] SETHURAM D，SRISAILAM S 和 PONANGI BR。经过新颖的两步奥氏体回火处理的合金奥氏体球墨铸铁的滑动磨损和腐蚀行为。眼压会议系列：材料科学与工程，2018，346（1）。 https://doi.org/10.1088/1757-899X/346/1/012035
[13] TARAN YN，UZLOV KI 和 KUTSOV AY。奥氏体球墨铸铁中的贝氏体反应动力学。物理学报，1997，7（5）。https://doi.org/10.1051/jp4:1997568
[14] KILICLI V. 和 ERDOGAN M. 具有双重基体结构的部分奥氏体和奥氏体球墨铸铁的应变硬化行为。材料工程与性能学报 2008，17（2）：240-249。https://doi.org/10.1007/s11665-007-9143-y
[15] SELLAMUTHU P，SAMUEL DGH，DINAKARAN D 等。奥氏体球墨铸铁（阿迪）：奥氏体温度对组织，机械和磨损性能以及能耗的影响。金属（巴塞尔），2018，8（1），53：1-12。 https://doi.org/10.3390/met8010053
[16] SAHIN Y，ERDOGAN M 和 KILICLI V。双矩阵结构的奥氏体球墨铸铁的磨损行为。材料科学与工程：一种，2007，444（1-2）：31-38。https://doi.org/10.1016/j.msea.2006.06.071
[17] DONG BX，QIU F，LI Q 等。纳米碳化钛的合成，结构，形貌表征及演化机理及其进一步的应用。纳米材料。2019，9（8）：1152. https://doi.org/10.3390/nano9081152
[18] ČATIPOVIĆ N，ŽIVKOVIĆ D 和 DADIĆ Z。钼和锰对奥氏体球墨铸铁力学性能的影响。技术公报，2018，25（2）：635-642。 https://doi.org/10.17559/TV-20170124120729
[19] WRAWRYNOWICZ，Z. 和 DYMSKI，S. 在阿迪的奥氏体反应过程中碳分配的分析。铸造工程档案，2008，8（3）：69-74。
[20] DAKRE V，PESHWE DR，PATHAK SU 等。通过两步奥氏体化工艺获得的奥氏体球墨铸铁的机械特性。印度金属学会学报 2017，70（9）：2381-2387。https://doi.org/10.1007/s12666-017-1099-5
[21] BOCCARDO AD，DARDATI PM，GODOY LA。合金元素分布对奥氏体球墨铸铁的影响。材料科学与技术（英国），2018，34（17）：2153-2165。https://doi.org/10.1080/02670836.2018.1521062
[22] CHENG H，FU H，MA S 等。奥氏体化工艺对卡氏体奥氏体球墨铸铁组织和性能的影响。材料研究快报，2019，6（1）。 https://doi.org/10.1088/2053-1591/aae44c
[23] MOZUMDER YH，BEHERA RK 和 SEN S. YH。临界奥氏体化温度，淬火介质和回火温度对双基体球墨铸铁力学性能和磨损行为的影响。奥里萨邦物理学报，2015，22（1）：39-51。
[24] TYRAŁA E，GÓRNY M，KAWALEC M 等。奥氏体球墨铸铁奥氏体回火过程中奥氏体体积分数的评价。金属（巴塞尔）。2019，9（8）。https://doi.org/10.3390/met9080893
[25] YANG J 和 PUTATUNDA SK。新型的两步奥氏体回火工艺对奥氏体球墨铸铁（阿迪）的应变硬化行为的影响。材料科学与工程：一种，2004，382（1-2）：265-279。https://doi.org/10.1016/j.msea.2004.04.076
[26] ARANZABAL J，SERRAMOGLIA G，GORIA CA 等。开发用于汽车悬架零件的新型混合（铁素体-奥氏体）球墨铸铁。国际铸造金属研究杂志，2003，16（1-3）：185-190，https://doi.org/10.1080/13640461.2003.11819580
x